RESEARCH PAPER

Effects of the antagomiRs 15b and 200b on the altered healing pattern of diabetic mice

Correspondence Professor Alessandra Bitto, Department of Clinical and Experimental Medicine, Torre Biologica 5th floor, c/o AOU Policlinico 'G. Martino', Via C. Valeria, 98125 Messina, Italy. E-mail: abitto@unime.it

Gabriele Pizzino[1], Natasha Irrera[1], Federica Galfo[1], Giovanni Pallio[1], Federica Mannino[1], Angelica D'amore[1], Enrica Pellegrino[1], Antonio Ieni[3], Giuseppina T Russo[1], Marco Calapai[1], Domenica Altavilla[2], Francesco Squadrito[1] and Alessandra Bitto[1] [iD]

[1]Department of Clinical and Experimental Medicine, Section of Pharmacology, Medical School, University of Messina, Messina, Italy, [2]Department of Biomedical Sciences, Dentistry and Morphological and Functional Images, University of Messina, Messina, Italy, and [3]Department of Human Pathology, University of Messina, Messina, Italy

BACKGROUND AND PURPOSE

Diabetic patients with non-healing ulcers have a reduced expression of VEGF. Genetically diabetic mice have an altered expression pattern of VEGF and its receptor, VEGF receptor 2 (VEGFR-2). In diabetic wounds, the microRNAs, miR15b and miR200b, which respectively inhibit VEGF and VEGF-R2 mRNAs, are up-regulated, further affecting the impaired angiogenesis. We investigated whether anti-miRs directed toward miR15b and miR200b could improve wound repair in genetically diabetic mice.

EXPERIMENTAL APPROACH

Skin wounds were produced on the backs of female diabetic mice. The anti-miRs (antimiR15b, antimiR200b or antimiR15b/200b) at 10 mg·kg^{-1}, or vehicle were applied to the wound edge. Mice were killed on days 7, 14 and at time of complete wound closure. Levels of mRNA and protein of angiogenic mediators and their receptors were measured with RT-qPCR and Western blotting. Wounds were examined by histological and immunochemical methods.

KEY RESULTS

mRNA expression of VEGF, VEGFR-2, angiopoietin-1 and its receptor TEK were evaluated after 7 and 14 days. Protein levels of VEGF and transglutaminase II were measured at day 7, while VEGFR-2 and Angiopoietin-1 were measured at day 14. Histological features and the time to achieve a complete wound closure were also examined. Treatment with the anti-miRs improved the analysed parameters and the co-treatment resulted the most effective.

CONCLUSION AND IMPLICATIONS

The results suggest that the inhibition of miR15b and miR200b may have a potential application in diabetes-related wound disorders.

Abbreviations

Ang-1, angiopoietin-1; miR, micro RNA; TEK, TK endothelial; VEGFR-2, VEGF receptor 2

Introduction

Alterations in vascular homeostasis due to endothelial dysfunction are considered one of the major features of diabetic vasculopathy, acting as pro-inflammatory/thrombotic factors that eventually lead to atherosclerosis.

Type 2 diabetic patients show an impaired wound healing and this defect together with diabetic neuropathy, hyperglycaemia and susceptibility to infections can easily lead to ulcer formation and even amputation (Falanga, 2005). Angiogenesis plays a pivotal role in wound healing and formation of new vessels, promoted by several biochemical factors such as **VEGF** and angiopoietin-1 (Ang-1), are required to properly support the healing process. Angiogenesis can be divided in three steps: resting, activation and resolution. In healthy tissues, endothelial cells are in the resting phase. When exposed to pro-angiogenetic factors, the endothelial cells are activated and start to proliferate, migrate and differentiate to form new blood vessels. To allow this process to occur, basal membrane has to be degraded, so that the sprouting can start. Endothelial cells grow and migrate following the leading tip cell, promoting the elongation of the new vessel. During the resolution phase, the structures of adjacent vessels can be fused together to form the new mature vessel. After that, a new basal membrane is synthesized, and the endothelial cells return to the resting phase (Johnson and Wilgus, 2014).

The best known pro-angiogenic factor is the protein VEGF, which plays a central role in angiogenesis both in embryos and in adult organisms. Its actions stimulate the different phases of angiogenesis and promote the survival of endothelial cells (Ferrara, 2009, 2010; Wietecha and Di Pietro, 2013; Johnson and Wilgus, 2014). VEGF binds to two different tyrosine-kinase receptors, **VEGFR-1** and **VEGFR-2**, the second one being more involved in activation of endothelial cells and angiogenesis. VEGFR-2 activates **PKB**, inhibiting apoptosis, and **MAPK**, thus stimulating proliferation (Ferrara, 2009, 2010; Wietecha and Di Pietro, 2013; Johnson and Wilgus, 2014).

Because of the decreased production of growth factors in diabetic peri-lesional tissues and to the increase in glycaemia, oxidative stress and ROS (which impair endothelial cells and fibroblasts metabolism), both angiogenesis and wound healing process are impaired (Russo *et al.,* 2011; Kim *et al.,* 2012; Peplow and Baxter, 2012; Hu and Lan, 2016). Recently, new mechanisms involved in wound healing regulation and impairment have been described. In particular, diabetic patients showed an altered expression of several micro RNAs (miRNAs; Assar *et al.,* 2016; Raffort *et al.,* 2015; Leeper and Cooke, 2011). miRNAs are short non-coding RNAs (single stranded, about 22 nt in length) which act as post-transcriptional regulators by binding the complementary 5′UTR of target mRNAs, thus inhibiting translation and promoting degradation of the target mRNA. miRNAs can bind several target mRNAs, thus orchestrating a complex pattern of regulation in several physiological and pathological conditions, such as inflammation, atherosclerosis, vasculitis and apoptosis of endothelial cells (Voglova *et al.,* 2016). The miRNA, miR15b (miRNA-15b), as well as miR200b (Chan *et al.,* 2011), act as negative modulators in angiogenesis (Poliseno *et al.,* 2006). The former (miR15b) binds VEGF and hypoxia inducible factor (HIF)-1α mRNA, thus decreasing production of these key pro-angiogenic mediators. In an *in vivo* model of wound healing, diabetic mice showed a dramatic increase in the concentration of miR15b in peri-lesional tissues, coupled with a reduced expression of its target genes (Xu *et al.*, 2014). On the other hand, miR200b targets, among other mRNAs, the mRNA coding for VEGFR-2 (Sinha *et al.*, 2015). There is experimental evidence showing that down-regulation of miR200b leads to an increase in the angiogenetic process, improving the wound healing process (Chan *et al.,* 2012).

Inhibition of miRNAs is a useful experimental tool but it has been also proposed, and has actually been used, as an experimental therapeutic strategy (Gandellini *et al.,* 2011). One way to achieve inhibition of specific miRNAs is to target them with short, anti-sense, nucleic acid which is complementary to each target miRNA. These molecules, called antagomiRs, can be used *in vivo*, and to achieve a better affinity for the target, they had been modified in several ways (Kaeuferle *et al.,* 2014). The most common and efficient modified antagomiRs are called locked nucleic acids (LNAs). These LNAs allow the targeting of more than one miRNA simultaneously, with high affinity for the target (Laganà *et al.,* 2014). This class of antagomiRs carries two methyl groups in the 2′-oxygen and 4′-carbon, forming a cyclic structure. This structural feature prevents the LNAs changing conformation (by keto-enolic tautomerisation), increases affinity for the target and decreases toxicity. The LNAs have been successfully used as experimental therapeutic strategy to rescue a disease-related molecular pathway affected by overexpression of miRNAs (Ishida and Selaru, 2013).

Taken together, these observations led us to consider the targeting, by antagomiRs, of miR15b and miR200b, as a therapeutic option to improve wound healing in leptin receptor-knock out diabetic mice.

Methods

Anti-miRs design

Anti-miRs have been designed to be inverse complementary to the respective miRNAs (miR15b and miR200b); the sequence of both miR15b and miR200b has been obtained from mirbase.org, miR15b: 5′-UAGCAGCACAUCCUGGUU UACA- 3′; and miR200b: 5′-CAUCUUACUGGGGCAGCAUU GGA-3′. Considering these sequences, we designed the two anti-miRs: anti-miR15b: 5′-UGUAAACCAGGAUGUGCUG CUA-3′; and anti-miR200b: 5′-UCCAAUGCUGCCCAGUAA GAUG-3′. We also designed two scrambled antagomiRs: 5′-GAAAUCAUUGGUCGCCGAUAGU-3′ (scramble for anti-mir-15b); and 5′-GGGCUUCAGCACUACGUUCAAA-3′ (scramble for anti-mir-200b). AntagomiRs and scrambles have been purchased from Exiqon (Vedbaek, Denmark), shipped as dry powder and re-suspended in RNAse-free water to a final concentration of 25 nM.

Animals and experimental procedures

All animal care and experimental procedures followed the Guide for the care and use of laboratory animals, eighth

edition (2011) (http://grants.nih.gov/grants/olaw/guide-for-the-care-and-use-of-laboratory-animals.pdf), as well as the Directive 63/2010/EU on the protection of animals used for scientific purposes and were approved by the Ethics Committee of Messina University. Animal studies are reported in compliance with the ARRIVE guidelines (Kilkenny et al., 2010; McGrath and Lilley, 2015).

C57BL/KsJ-m+/+ Lepr^{db} (db$^+$/db$^+$) female diabetic mice (n = 83; 10 weeks old at the beginning of the experiment) and C57/Bl6J female healthy mice (n = 7) were purchased from Charles River (Calco, Italy). Diabetic animals weighed 30–35 g while normoglycaemic animals weighed 22–25 g. Animals have been kept at the Animal Facility of the Department of Clinical and Experimental Medicine under controlled environmental conditions (12 h day–night cycles, 23–24°C), housed five or seven per cage (depending on group allocation), in plastic cages with conventional bedding, and provided with food and water ad libitum and the proper enrichment.

The wound healing model and the specific strain have been chosen in accordance with our previously published papers (Galeano et al., 2004, 2008; Bitto et al., 2008, 2013, 2014). After general anaesthesia (ketamine and xylazine 80 and 10 mg·kg^{-1}, respectively, i.p.), animals were shaved on the back, and the skin cleaned with iodine solution for asepsis. Incisional wounds were performed as follows: two longitudinal incisions (3 cm in length) were produced with a sterile scalpel and then sutured with sterile 4–0 silk, as previously reported (Galeano et al., 2004, 2008; Bitto et al., 2008, 2013, 2014). To accelerate recovery, animals received 500 μL of 0.9% NaCl i.p., and to provide analgesia, 0.5% bupivacaine (8 mg·kg^{-1}) was administered intradermally for the first 3 days following surgery. No animals were killed for humane reasons, i.e., experiencing pain or infections at the wound site. The only reported clinical sign of discomfort was scratching at the site of the stitches.

Animals (10 in each group) were randomized to receive a single dose of anti-miR15b (10 mg·kg^{-1} in 0.9% NaCl); anti-miR200b (10 mg·kg^{-1} in 0.9% NaCl); both anti-miR15b and anti-miR200b; or vehicle alone (0.9% NaCl). Mice (five per group) treated with scramble-anti-miR15b (10 mg·kg^{-1} in 0.9% NaCl), or scramble-anti-miR200b (10 mg·kg^{-1} in 0.9% NaCl) or both scramble-anti-miRs were used only for the 7 days evaluation. Anti-miRs and scramble-anti-miRs were injected peri-lesionally, in a final volume of 200 μL. The suspension was injected at the four cardinal points of the wound, so each point received roughly 50 μL of the total volume.

Before killing, blood glucose levels were assessed with the Multicare instrument (2Biological Instruments, Besozzo, Italy) with a detection range of 0.25–5 g·L^{-1}. Five mice from each group receiving the anti-miRs were killed 7 and 14 days after the surgical procedure. All mice that received the scramble anti-miRs were killed at day 7. One of the incisions (from each animal) was collected for molecular analyses, the other one to carry out histology and immunohistochemistry.

To evaluate the time of complete wound closure, we performed an excisional wound on another set of 28 diabetic and 7 normoglycaemic mice. In brief, a circular piece (1 cm diameter) of cutaneous tissue was removed, from the shaved back of diabetic animals using a biopsy punch. Animals were then randomized (seven in each group) to receive anti-miRs or vehicle as described above and killed at the time of complete wound closure. Normoglycaemic mice received vehicle treatment.

RT-qPCR

Total RNA was extracted from skin samples (70 mg) using Trizol reagent (Thermo Fisher Scientific, Waltham, MA, USA), following the manufacturer's protocol, and was quantified with a spectrophotometer (NanoDrop Lite; Thermo Fisher Scientific). Reverse transcription was carried out using 1 μg of RNA by using the SuperScript® VILO™ cDNA synthesis kit (Thermo Fisher Scientific) and random primers, following the manufacturer's protocol. One microlitre of total cDNA was used to quantify VEGF (catalogue number: mm01281449_m1), VEGFR-2 x(catalogue number: mm01222421_m1), Ang-1 (catalogue number: mm00456503_m1) and TK endothelial (TEK; catalogue number: mm01256894_m1) by Real-Time qPCR, using β-actin (catalogue number: 4352341E; Life Technologies) as the reference gene. Reactions have been carried out in singleplex in 96-well plates using the TaqMan Universal PCR master mix and pre-made hydrolysis probes (Thermo Fisher Scientific). The PCR reaction was monitored by using the QuantStudio 6 Flex (Thermo Fisher Scientific), and results were quantified by the $2^{-\Delta\Delta Ct}$ method for both target and reference genes. The unwounded skin from diabetic animals was used to provide calibrator samples.

Western blot analysis

After removal of skin samples, proteins were extracted and stored at −20°C until analysis, as previously described (Bitto et al., 2013). Separated proteins were blocked with 5% non-fat dry milk in TBS-0.1% Tween for 1 h at room temperature then incubated with a primary antibody for VEGF-A (Abcam, Cambridge, UK), Ang-1, Transglutaminase-2 (Millipore, Temecula, CA, USA) or β-actin (Cell Signalling, Beverly, MA, USA), in TBS-0.1% Tween overnight at 4°C. Following incubation, antibody was removed, and membranes were incubated with secondary peroxidase-conjugated antibodies (Thermo Fisher Scientific, Waltham, MA, USA) for 1 h at room temperature. Protein signals were observed by the enhanced chemiluminescence system and quantified by scanning densitometry by using a blot scanner (C-DiGit, LiCor, Lincoln, NE, USA). Samples were coded, and the experiments were repeated three times. Results were expressed as integrated intensity compared with those of control animals measured within the same batch and normalized to β-actin for each sample, to reduce variance.

Histological examination and time to complete wound closure

Wound samples were fixed in 10% neutral buffered formalin and processed as previously described (Bitto et al., 2013, 2014). Haematoxylin/eosin or Masson's trichrome stain were performed on coded samples. All slides were examined, by means of an eyepiece grid under the microscope from ×20 to ×100 magnification, by a pathologist, blinded to the treatments. The following parameters were evaluated and scored: re-epithelialization, dermal matrix deposition and regeneration, granulation tissue formation and remodelling. The histological specimens were evaluated according

to the score as described by Bitto *et al.,* (2013, 2014). The time to complete wound closure, as shown by a closed linear healing ridge, was monitored as described previously (Bitto *et al.,* 2014).

Immunohistochemistry

Paraffin-embedded tissues were sectioned (5 μm) and re-hydrated, and antigen retrieval was performed using 0.05 M sodium citrate buffer as previously described (Bitto *et al.,* 2013). Slides were incubated overnight with primary antibodies to detect CD-31 (Abcam) and VEGFR-2 (Cell Signalling). 3-3′ Diaminobenzidine (Sigma, St Louis, MO, USA) was used to reveal the reaction and counterstain was performed with haematoxylin where needed.

To assess new blood vessel formation, microvessel density was estimated after CD-31 staining. Briefly, three hot spots or areas with the highest visible blood vessel density (marked by CD31) per section were selected, in the dermis just proximal to the wound site, and the number of small calibre blood vessels having a visible lumen were counted per high-power field (×40 magnification) by three pathologists, unaware of the treatments.

Breaking strength

At day 12, the maximum load (breaking strength) tolerated by wounds was measured blindly on coded samples using a calibrated tensometer (Sans, Milan, Italy) as previously described (Bitto *et al.,* 2013). The ends of the skin strip were pulled at a constant speed (20 cm·min^{-1}), and breaking strength was expressed as the mean maximum level of tensile strength in newtons (N) before separation of wounds.

Data and statistical analysis

The data and statistical analysis in this study comply with the recommendations on experimental design and analysis in pharmacology (Curtis *et al.,* 2015). An *a priori* power calculation was performed to define the number of animals needed in each group, using as primary endpoint the variation of VEGF mRNA levels based on our previous study (Bitto *et al.,* 2008), with an α of 0.05 and a power of 90%.

All data were expressed as means ± SD. Comparisons between different treatments were analysed by one-way ANOVA followed by Tukey's multiple comparison test when F achieved <0.05 and there was no significant variance
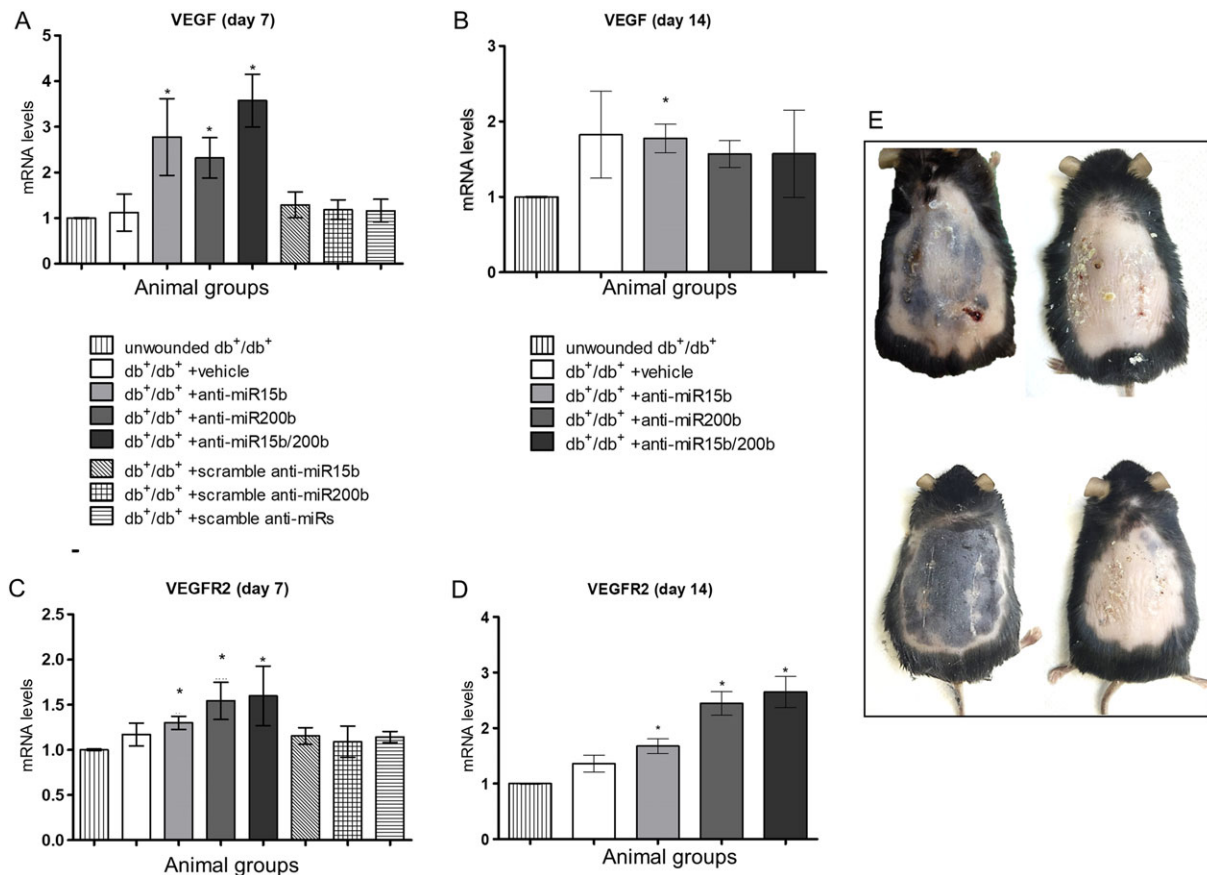

Figure 1

Expression of the mRNA for VEGF and VEGFR-2 in skin tissue, quantified by RT-qPCR at both 7 (A, C) and 14 days (B, D) after surgical procedures. Each bar represents the mean ± SD of five animals. *$P < 0.05$, significantly different from db$^+$/db$^+$ + vehicle. Panel (E) represents the appearance of wounds at day 14 after removal of the stitches and before excision. Examples (from top left clockwise) are of db$^+$/db$^+$ + vehicle, db$^+$/db$^+$ + anti-miR15b, db$^+$/db$^+$ + anti-miR200b and db$^+$/db$^+$ + anti-miR15b/200b mice.

inhomogeneity. In all cases, a probability error of less than 0.05 was selected as the criterion for statistical significance. Statistical analyses were performed using SPSS 20.0 software for Windows. Graphs were drawn using GraphPad Prism (version 5.0 for Windows).

Nomenclature of targets and ligands

Key protein targets and ligands in this article are hyperlinked to corresponding entries in http://www.guidetopharmacology.org, the common portal for data from the IUPHAR/BPS Guide to PHARMACOLOGY (Southan *et al.,* 2016), and are permanently archived in the Concise Guide to PHARMACOLOGY 2017/18 (Alexander *et al.,* 2017a,b).

Results

VEGF and VEGFR-2 expression in wounds

Wounds from diabetic mice treated with anti-miR15b, anti-miR200b and anti-miR15b/200b demonstrated an increased expression of VEGF (Figure 1A) and VEGFR-2 (Figure 1C, D), compared with that in vehicle-treated animals, demonstrating the efficacy of the anti-miRs against the corresponding miRNAs. The effect on VEGF was more evident at day 7 after wounding, rather than at day 14 (Figure 1B), while VEGFR-2 mRNA was more clearly affected at day 14. These results also suggest that a single anti-miR injection was able to inhibit miRNAs for at least 14 days. None of the scrambles used as control, administered either alone or in combination, showed any effect on target genes (Figure 1A). As shown in

Figure 1E, the vehicle-treated animal still had a scab and some small ulcerations at the wound site at day 14, while treated animals showed no signs of ulceration and in the case of the double anti-miR treatment there was no sign of a scab, demonstrating the improved healing.

Angiopoietin-1 and TEK expression in wounds

At days 7 and 14 post-wounding, Ang-1 and its receptor TEK (or Tie-2) mRNA expression were also evaluated, because Ang-1 is a known target of miR200b. Mice treated with anti-miR15b showed a modest increase in Ang-1 and TEK, particularly at day 7. Treatment with anti-miR-200b and the combination of anti-miR15b/200b demonstrated a robust expression of Ang-1 (Figure 2A, B) and TEK (Figure 2C, D) in treated animals, especially at day 14.

VEGF, angiopoietin-1 and VEGFR-2 protein expression

Because of the maximum observed effects on mRNA, VEGF protein expression was evaluated at day 7, and that of Ang-1 and VEGFR-2 at day 14 (Figure 3). Mice treated with anti-miR15b, anti-miR200b and anti-miR15b/200b demonstrated an increased expression of VEGF (Figure 3A) in wounds, compared with vehicle treated mice. The most significant effect was observed using both anti-miRs together. The maximum increase in Ang-1 protein expression was observed with anti-miR-200b alone or in combination (Figure 3B). In order to highlight the endothelial cells expressing the receptor in the dermis, where tissue
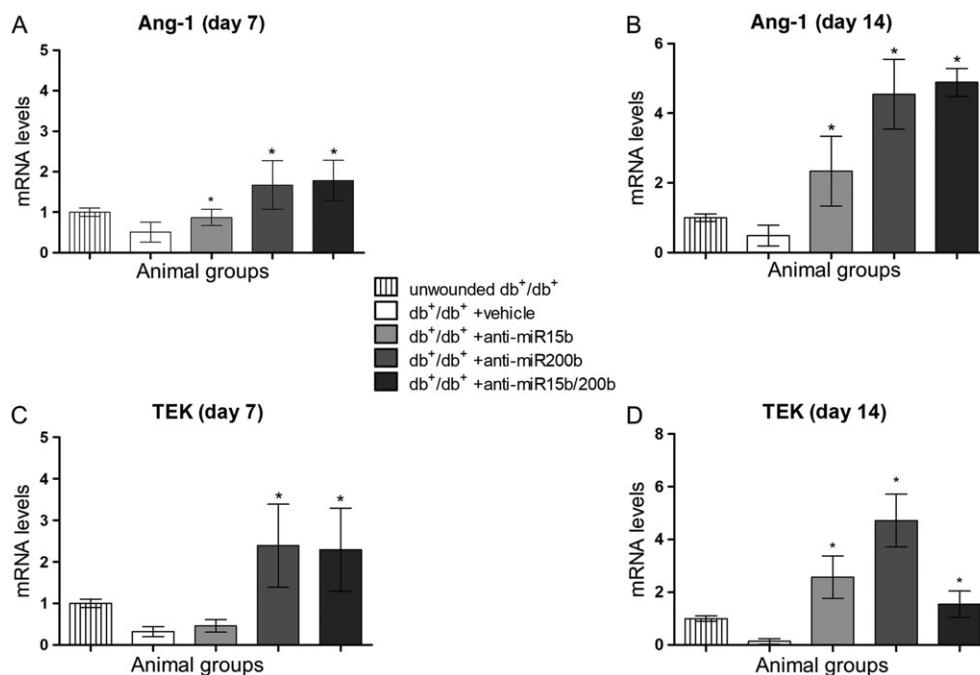

Figure 2

Ang-1 and TEK mRNA expression in skin tissue, quantified by RT-qPCR at both 7 (A, C) and 14 days (B, D) after surgical procedures. Each bar represents the mean ± SD of five animals. *$P < 0.05$, significantly different from db$^+$/db$^+$ + vehicle.
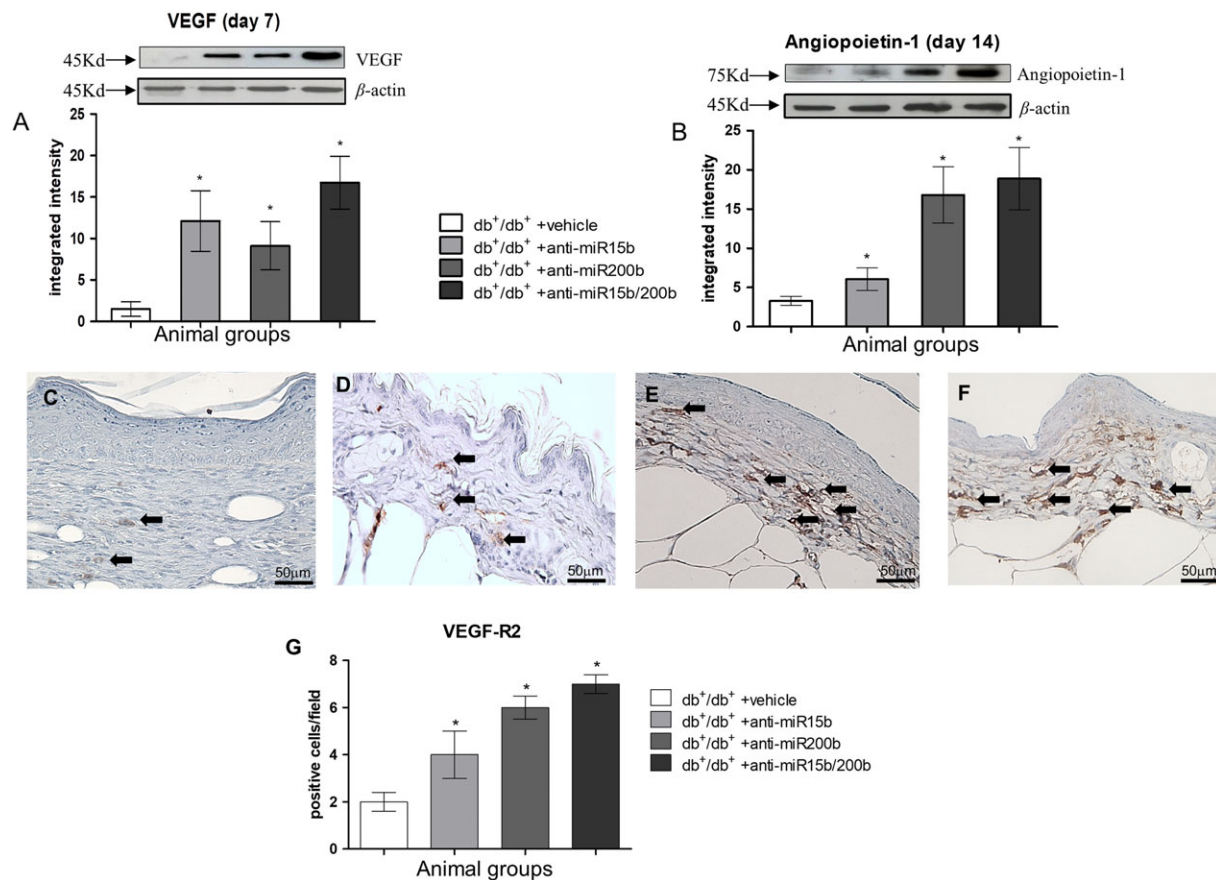
Figure 3

VEGF (A) and Ang-1 (B) protein expression quantified by Western blot 7 and 14 days after wounding respectively. Each bar represents the mean ± SD of five animals. *$P < 0.05$, significantly different from db+/db+ + vehicle. VEGFR-2 protein was assayed at day 14, by immunohistochemistry (C–F); arrows point at positive small vessels in the dermis with a visible lumen. (C) db+/db+ + vehicle; (D) db+/db+ + anti-miR15b; (E) db+/db+ + anti-miR200b; (F) db+/db+ + anti-miR15b/200b. (G) The graph represents mean VEGFR-2 expression for each group. Each bar represents the mean ± SD of five animals. *$P < 0.05$, significantly different from versus db+/db+ + vehicle.

restoration takes place, VEGFR-2 expression was assessed by immunohistochemistry (Figure 3C–F). Increased staining was observed in small vessels, and the most significant effect was obtained in animals treated with anti-miR200b or the combination of anti-miR15b/200b.

Histological features and tissue remodelling

Histological evaluations were performed 7 and 14 days following wounding. At day 7, an abundant infiltration of inflammatory cells, erythrocytes in peri-lesional dermal tissue and haemorrhagic scab were observed in vehicle-treated mice (Figure 4A, E). Moreover, most of the histological samples showed a complete separation between the two epidermal edges. Animals treated with anti-miR15b (Figure 4B, E) showed a reduced inflammatory infiltrate and a partially closed epidermal edge. Wounds treated with anti-miR200b (Figure 4C, E) showed a completely restored epithelial edge, although the scab was still present and granulation tissue was not abundant. Treating the animals with the combination of anti-miR15b and anti-miR200b resulted in almost complete recovery of the basal

membrane, absence of the haemorrhagic scab and abundant granulation tissue (Figure 4D, E). Tissue remodelling at day 7 was also evaluated by Western blot that showed an increased expression of transglutaminase-2 (Figure 5A) that promotes the extracellular matrix-VEGF binding, in animals treated with the anti-miRs, consistent with an increased deposition of collagen tissue at the wound site (Figure 5B–E). In particular, treatment with anti-miR200b also improved formation of elastin fibres, as shown by the red staining obtained by Masson's trichrome (Figure 5D, E). In detail, the wound edges were still clearly visible at day 7 in anti-miR15b treated animals (Figures 4B and 5C), whereas a restored epithelial surface was clearly visible in anti-miR200b (alone or in combination) treated animals (Figures 4C, D and 5D, E).

At day 14, vehicle-treated animals (Figure 6A, E) showed a still incomplete epithelial rime and disorganized granulation tissue. Treatment with anti-miRs (Figure 6B–E) significantly improved the histological picture, and the most impressive effect was obtained treating the mice with both anti-miRs (Figure 6D, E). In detail, sebaceous glands and hair follicles
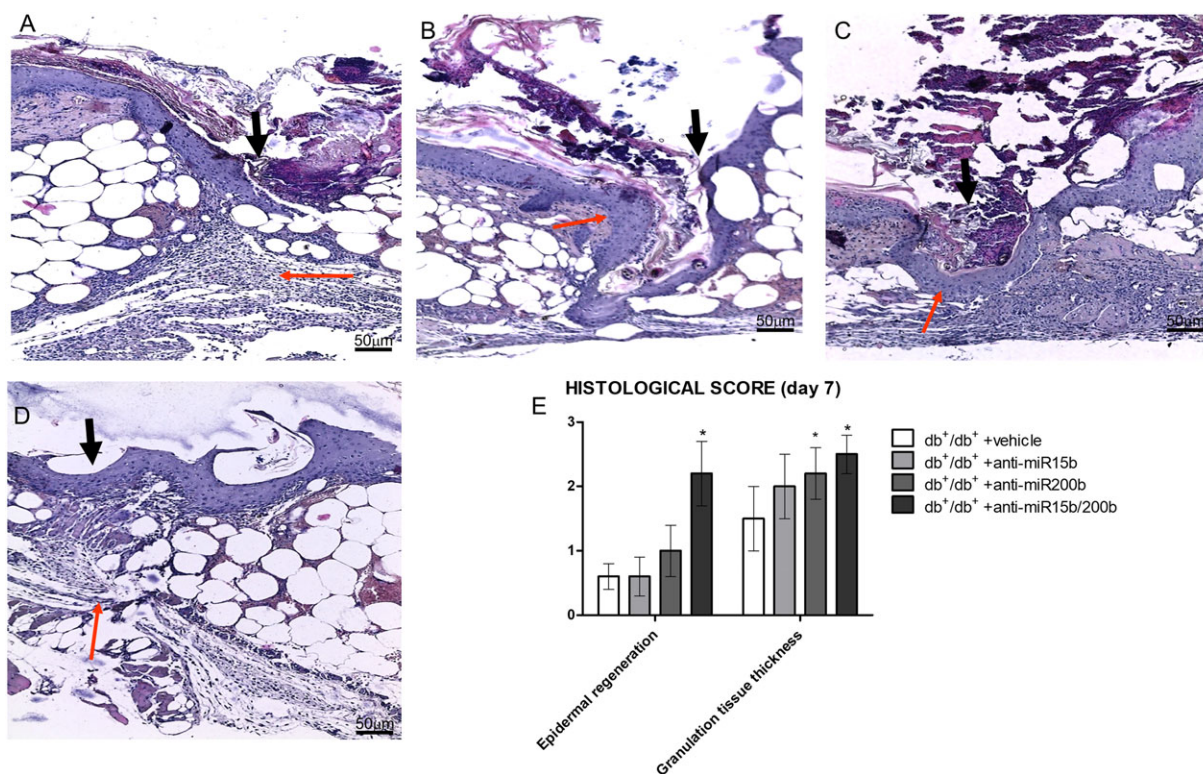
Figure 4

Haematoxylin-eosin staining of peri-lesional skin tissue from diabetic animals treated with vehicle (A), anti-miR15b (B), anti-miR200b (C) and anti-miR15b/200b (D), 7 days after surgical procedures. Black arrows point at the incision site, and red arrows point at granulation tissue. The graph represents the cumulative histological score for each group. Each bar represents the mean ± SD of five animals. $*P < 0.05$, significantly different from db$^+$/db$^+$ + vehicle.

were evident in dermal space in animals treated with anti-miRs (Figure 6B–D).

Tensile strength, evaluated at day 14 as a measure of the quality of the newly formed tissue, showed a marked increase in anti-miRs-treated animals compared to vehicle-treated ones (Figure 6F). The most effective treatment was the combination of anti-miR15b and anti-miR200b.

Angiogenesis

To confirm neo-angiogenesis, CD31 immunostaining was performed at day 14 (Figure 7). Positive staining of endothelial cells of small calibre vessels and single mesenchymal elements (possibly endothelial progenitors) in dermis demonstrated that mice treated with anti-miRs had a higher number of positive cells (Figure 7B–D) compared with vehicle-treated animals (Figure 7A, E). The count of positive cells defining a small vessel with a visible lumen (Figure 7E) shows that the greatest effect was obtained with the anti-miR15b/200b treatment.

Time to wound closure and safety assessment

Wounds were defined as closed when the epithelial tissue was completely restored in the area surrounding the incision, and the scab was absent. In vehicle-treated diabetic animals, time to wound closure was double that in normoglycaemic animals (Figure 8A). However all treatments with anti-miRs in

diabetic animals decreased the time needed to heal, with the shortest time following treatment with the combined anti-miR (Figure 8A). To assess if local administration of anti-miRs could reach the systemic circulation and target other tissues, we measured glycaemia (Figure 8B) and the expression of VEGF mRNA in liver (Figure 8C, D). No differences were observed between groups.

Discussion

The most effective, high-affinity anti-miRNA oligonucleotides designs rely on highly modified, synthetic oligonucleotide chemistries as LNAs. LNAs contain a methylene bridge between the 2′-O and 4′C of ribose to 'lock' it into a configuration that is optimal for hybridization. LNAs are also highly resistant to nuclease degradation, thus are ideal for *in vivo* use. Consequently, LNA-based anti-miRNAs show higher anti-miR activity at lower doses compared with the equivalent antagomir (Obad *et al.*, 2011). These features can explain the long-lasting effect observed in our experimental model. This strategy to dis-inhibit the normal expression of VEGF and other factors, rather than to increase their production pharmacologically, is of particular importance in a translational context, as it could limit the unwanted side effects related to increased angiogenesis in other tissues (Wahl *et al.*, 2004). Neoangiogenesis is an important process
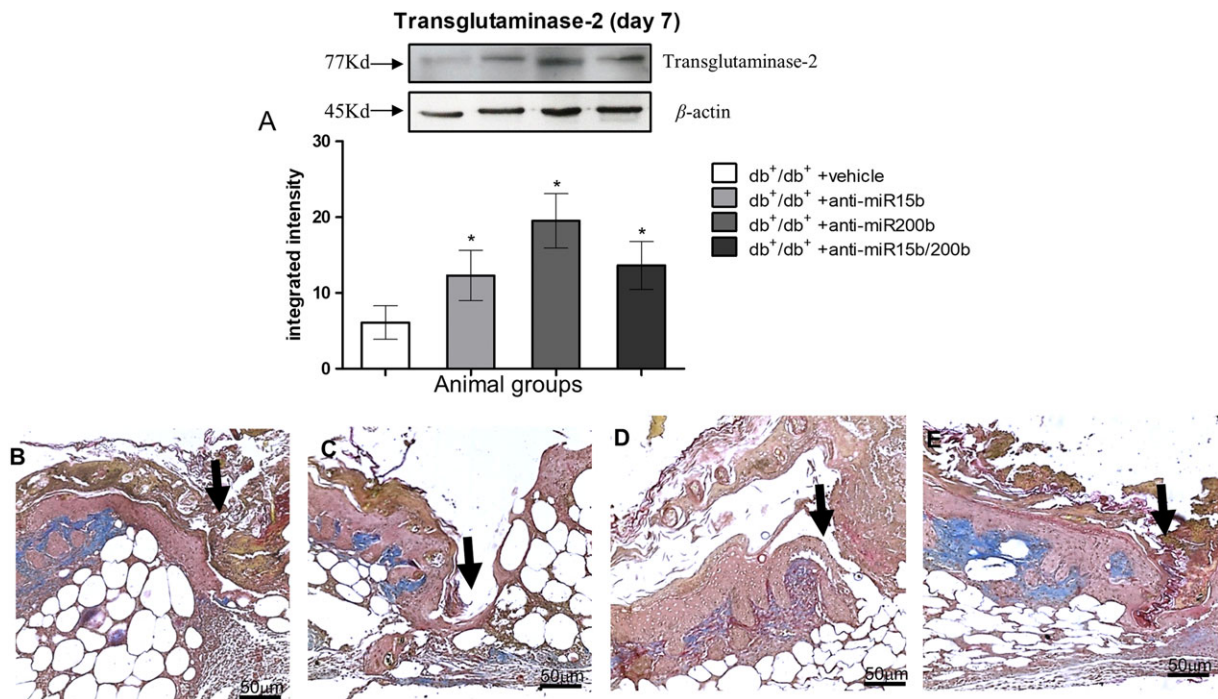
Figure 5

Transglutaminase-2 protein (A) quantification by Western blot from skin tissue at day 7 following wounding. Each bar represents the mean ± SD of five animals. *$P < 0.05$, significantly different from db^+/db^+ + vehicle. Masson's trichrome stain (B–E) was used to highlight sub-epithelial connective tissue restoration, (B) db^+/db^+ + vehicle; (C) db^+/db^+ + anti-miR15b; (D) db^+/db^+ + anti-miR200b; (E) db^+/db^+ + anti-miR15b/200b. Black arrows point at the incision site, blue colour stains collagen tissue with elastin (red stained fibres close to collagen).

involved in wound healing. The new vessels, formed after the inflammatory phase, bring oxygen and nutrients necessary to restore the integrity of damaged cutaneous tissue. One of the most important mediators of angiogenesis is VEGF and this growth factor is present in high concentration into the area surrounding the lesion. It is also produced by a wide range of cell types, including keratinocytes, macrophages and fibroblasts. Previous *in vivo* studies from our group showed that wound healing process may be accelerated and improved when VEGF production is increased (Bitto *et al.,* 2008, 2013, 2014; Galeano *et al.,* 2008). On the other hand, when VEGF is down-regulated, wound healing is impaired and a longer time is needed to restore the injured tissue completely (Johnson and Wilgus, 2014). In the last few years, new molecular mechanisms involved in impaired angiogenesis of diabetic patients have been identified and, in particular, an increase in specific miRNAs seems to affect the physiopathological features of diabetes (Raffort *et al.,* 2015). The miRNAs miR15b and miR200b are negative modulators in angiogenesis, inhibiting the processing of VEGF and VEGFR-2 mRNAs. Both these miRNAs are up-regulated in ulcerated tissue from diabetic mice (Chan *et al.,* 2011; Xu *et al.,* 2014). These observations lead us to consider an antagomiR-based targeting of miR15b and miR200b as a therapeutic approach to restore the angiogenetic process in diabetic mice. In our experimental conditions, anti-miR15b and anti-miR200b treatment improved the healing process, increasing the amount of new blood vessels in peri-lesional tissue,

restoring, at least in part, the impaired VEGF pathway. Treatment with anti-miRs also increased the levels of transglutaminase-2, which is required to bind VEGF to the ECM and trigger the VEGF-VEGFR-2 signalling pathway. In turn, this mechanism leads to an increase in collagen deposition and organization in the healing wound (allowing also elastin deposition), and this positive feedback-loop improved the histological features and the quality of the regenerated skin tissue, as showed by the increase of the maximum tolerated load. At 14 days, an increased expression of Ang-1 was observed, especially with anti-miR200b alone or in co-administration and this could be due to the fact that Ang-1 mRNA is a specific target of miR200b (Wang *et al.,* 2017). Ang-1 decreases during the early stages of angiogenesis, thus destabilizing the vessels so that the endothelial cells are able to start sprouting (Staton *et al.,* 2010) and, later on, its expression has to increase so that newly formed vessels are stabilized. Treatment with anti-miR200b alone, or combined with anti-miR15b, also improved the histological features at day 14, supported by an increased angiogenesis (as shown by microvascular density) and eventually by a reduced time to complete wound closure. From our data, it appears that anti-miR200b, alone or combined with anti-miR15b, had the greater effect, probably because increasing both VEGFR-2 and Ang-1 expression not only activates angiogenesis but also guarantees the integrity of the cascade of events that lead to the formation of new vessels. miR200b inhibition or ablation was also reported to improve pancreatic beta cell survival and to reduce oxidative
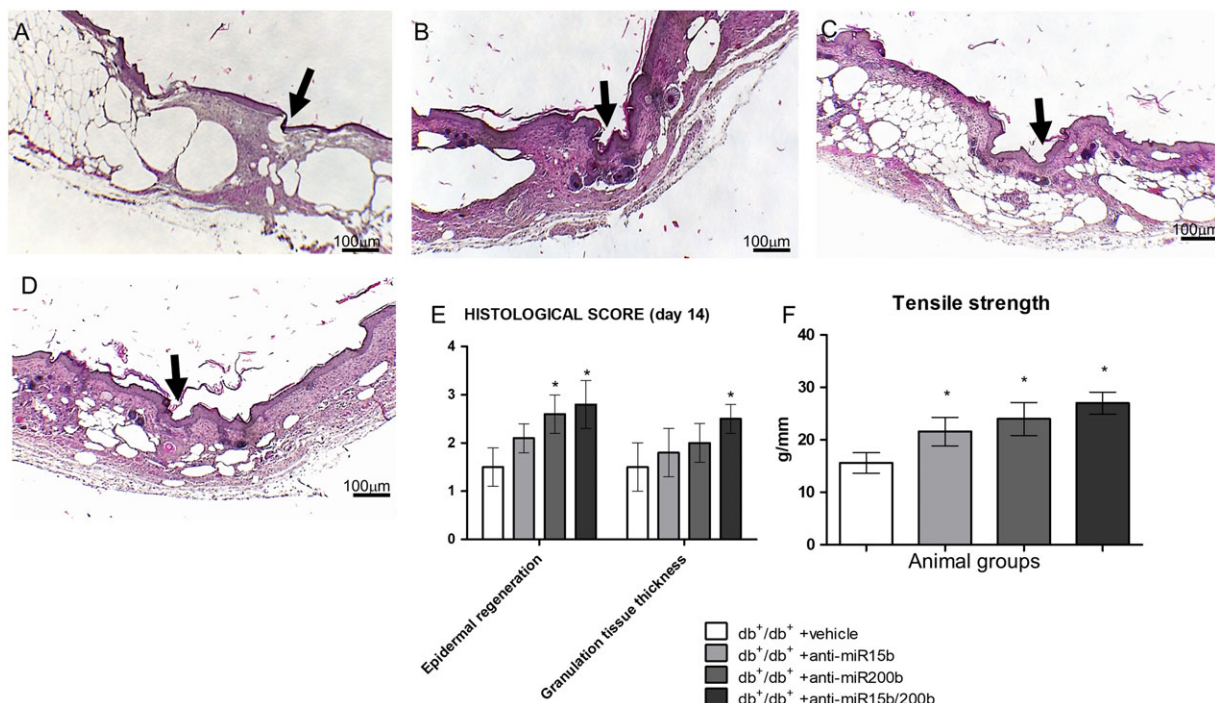
Figure 6

Haematoxylin-eosin staining of peri-lesional skin tissue from diabetic animals treated with vehicle (A), anti-miR15b (B), anti-miR200b (C) and anti-miR15b/200b (D), 14 days after surgical procedures. Black arrows point at the incision site. The graph (E) represents the cumulative histological score for each group. The graph (F) represents the wound's maximum tolerated strength recorded at day 14 post-wounding. Each bar represents the mean ± SD of five animals. *$P < 0.05$, significantly different from db$^+$/db$^+$ + vehicle.
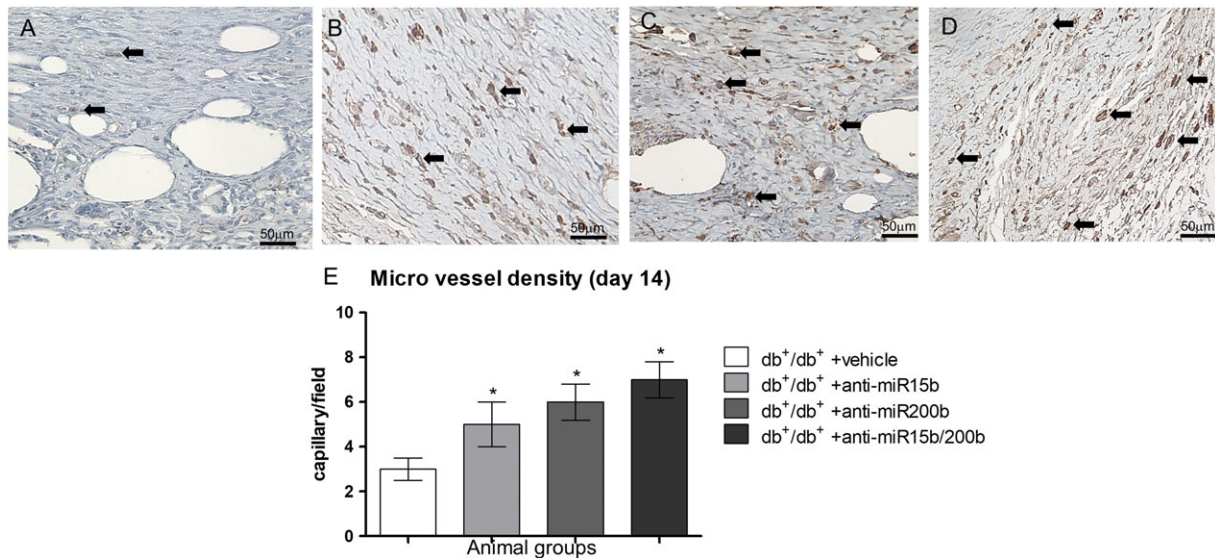

Figure 7

CD31 immunostaining (A–D) of wounded skin obtained at day 14; microphotographs are representative of diabetic animals treated with vehicle (A), anti-miR15b (B), anti-miR200b (C) and anti-miR15b/200b (D). The graph (E) represents the count of small vessels with visible lumen. Each bar represents the mean ± SD of five animals. *$P < 0.05$, significantly different from db$^+$/db$^+$ + vehicle.

stress in the same strain of mice used in our experiment (Belgardt *et al.*, 2015). However, we did not observe an improvement of glycaemia in our animals possibly because the locally administered anti-miR did not reach the systemic circulation, as also demonstrated by the unchanged levels of VEGF mRNA in the liver of treated animals.
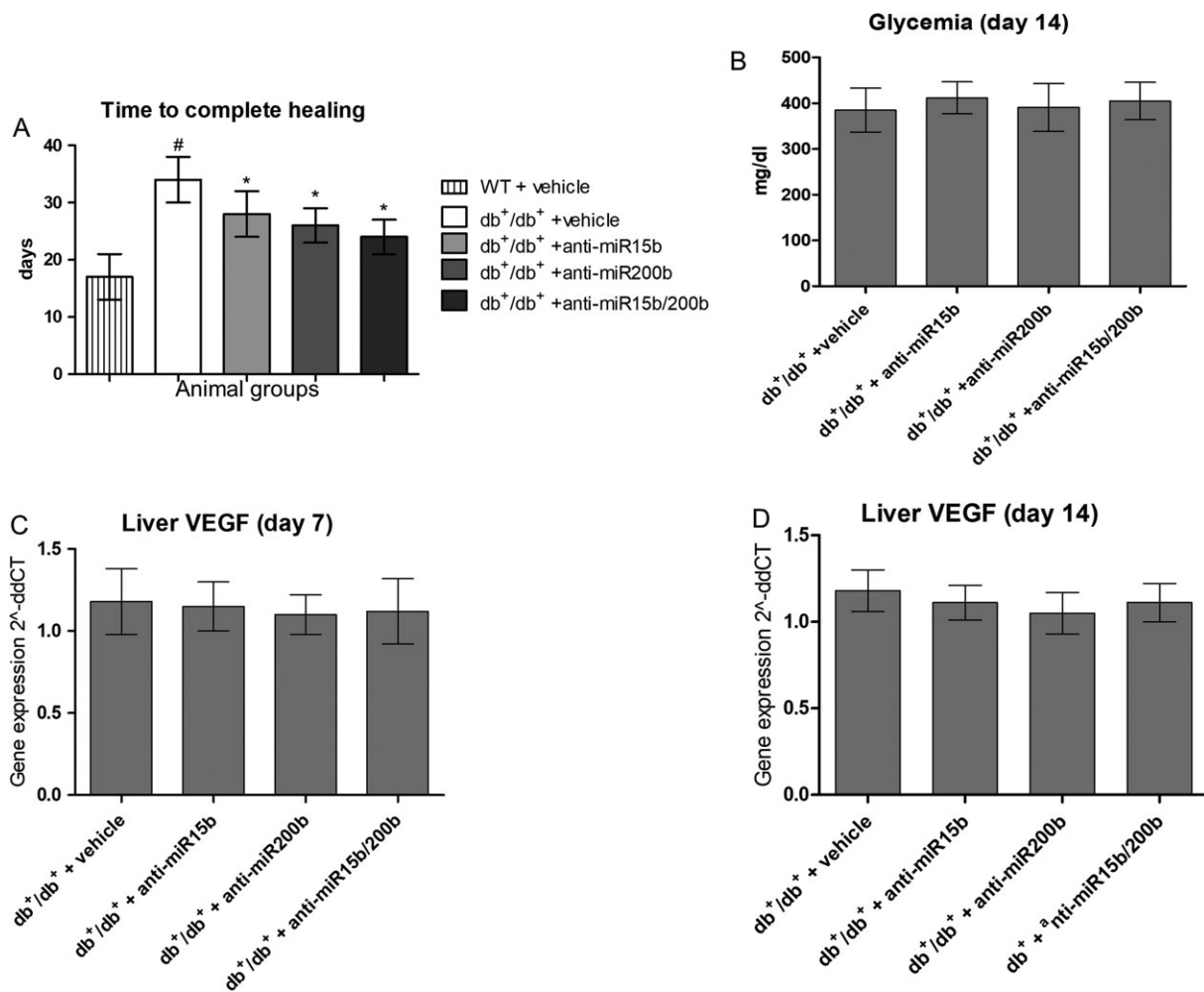
Figure 8

Time to complete healing (A) was assessed, in order to confirm that treatments were able to significantly improve this parameter. Each bar represents the mean ± SD of seven animals. #$P < 0.05$, significantly different from WT + vehicle; *$P < 0.05$, significantly different from db$^+$/db$^+$ + vehicle. Panel (B) shows glycaemic values for each group of animals 14 days after surgery, in order to check that our experimental findings were not affected by a remission of hyperglycaemia. Panels (C) and (D) show VEGF mRNA expression in liver 7 days (C) and 14 days (D) after surgery, to exclude systemic effects of our treatments. Each bar represents the mean ± SD of five animals.

Gene expression data showed that our anti-miRs together increased VEGF, Ang-1 and its receptor (Tek), and it is worth noting that, even if mRNA levels were not markedly affected by anti-miRs, the protein production increased as a result of a reduction in miRNA-mediated mRNA degradation. On the other hand, our results did not show that anti-miRs can also increase production of mRNA, a possible explanation of our observation of an increase in protein levels that was not always matched by the corresponding mRNA. The increase in Ang-1 and Tek is not surprising, as HIF-1α increases their transcription (Krock et al., 2011) and miR15b targets HIF-1α mRNA, while miR200b specifically targets Ang-1 mRNA (Wang et al., 2017), It is therefore very likely that the combined inhibition of the two miRNAs caused the observed increase.

Stimulation of angiogenesis could also represent a negative event in tissues such as retina, liver and brain. For example, those drugs that stimulate angiogenesis in diabetic patients, also present side effects derived from unwanted formation of new blood vessels (Wahl et al., 2004). Additionally, stimulation of angiogenesis can also affect precancerous states and undetected cancers (Shibuya, 2006). In light of these considerations, we assessed the systemic effects of our treatments by measuring VEGF mRNA expression at day 7 in liver and found no changes. This ruled out, at least in our experimental conditions, the possibility that locally administered anti-miRs can exert undesired systemic effects. These data may have important clinical implications, as antagomiRs could be used in the near future as local treatment for non-healing wounds. In spite of all these encouraging observations, the final healing time of diabetic wounds treated with the two anti-miR was almost 7 days longer than in wild-type mice. This incomplete return to normal levels of healing is probably due to the many other factors contributing to delayed healing, besides angiogenesis. Protein glycation and hyperglycaemia, together with

increased oxygen radicals, all contribute to the establishment of non-healing wounds (Peppa and Raptis, 2011; Catrina and Zheng, 2016), and a single approach that could target all these factors is far from being found. Thus, although the current approaches may target only one or just a few pathways at a time, angiogenesis is certainly one of the most important components of healing.

In conclusion, our data provide evidence that anti-miRs have an interesting profile in terms of both efficacy and safety, in their LNA™-enhanced form. Their local effects seem to be also long lasting, considering we gave only one injection of the anti-miRs, at the start of the healing process which lasted for 2-3 weeks. Nonetheless, further studies are needed to fully elucidate the exact mechanism(s) of action of these anti-miRs, as well as their viability as potential therapeutic options in pathological conditions involving impaired angiogenesis.

Acknowledgements

Authors contributions

G.P., A.B. and F.S. conceived the experiment. N.I., F.G., G.Pa., F.M., A.D., E.P., A.I. and M.C. researched data. G.P., A.B., G.T.R. and D.A. analysed data. G.P. and A.B. drafted the paper. All authors critically revised and approved the final version of the manuscript. All authors agree to be accountable for all aspects of the work in ensuring that questions are related to the accuracy or integrity of any part of the work.

Conflict of interest

The authors declare no conflicts of interest.

Declaration of transparency and scientific rigour

This Declaration acknowledges that this paper adheres to the principles for transparent reporting and scientific rigour of preclinical research recommended by funding agencies, publishers and other organisations engaged with supporting research.

References

Alexander SPH, Fabbro D, Kelly E, Marrion NV, Peters JA, Faccenda E *et al*. (2017a). The Concise Guide to PHARMACOLOGY 2017/18: Catalytic receptors. Br J Pharmacol 174: S225–S271.

Alexander SPH, Fabbro D, Kelly E, Marrion NV, Peters JA, Faccenda E *et al*. (2017b). The Concise Guide to PHARMACOLOGY 2017/18: Enzymes. Br J Pharmacol 174: S272–S359.

Assar ME, Angulo J, Rodríguez-Mañas L (2016). Diabetes and ageing-induced vascular inflammation. J Physiol 594: 2125–2146.

Belgardt BF, Ahmed K, Spranger M, Latreille M, Denzler R, Kondratiuk N *et al*. (2015). The microRNA-200 family regulates pancreatic beta cell survival in type 2 diabetes. Nat Med 21: 619–627.

Bitto A, Minutoli L, Altavilla D, Polito F, Fiumara T, Marini H *et al*. (2008). Simvastatin enhances VEGF production and ameliorates impaired wound healing in experimental diabetes. Pharmacol Res 57: 159–169.

Bitto A, Irrera N, Minutoli L, Calò M, Lo Cascio P, Caccia P *et al*. (2013). Relaxin improves multiple markers of wound healing and ameliorates the disturbed healing pattern of genetically diabetic mice. Clin Sci (Lond) 125: 575–585.

Bitto A, Altavilla D, Pizzino G, Irrera N, Pallio G, Colonna MR *et al*. (2014). Inhibition of inflammasome activation improves the impaired pattern of healing in genetically diabetic mice. Br J Pharmacol 171: 2300–2307.

Catrina SB, Zheng X (2016). Disturbed hypoxic responses as a pathogenic mechanism of diabetic foot ulcers. Diabetes Metab Res Rev 32 (Suppl 1): 179–185.

Chan YC, Khanna S, Roy S, Sen CK (2011). miR-200b targets Ets-1 and is down-regulated by hypoxia to induce angiogenic response of endothelial cells. J Biol Chem 286: 2047–2056.

Chan YC, Roy S, Khanna S, Sen CK (2012). Downregulation of endothelial microRNA-200b supports cutaneous wound angiogenesis by desilencing GATA binding protein 2 and vascular endothelial growth factor receptor 2. Arterioscler Thromb Vasc Biol 32: 1372–1382.

Curtis MJ, Bond RA, Spina D, Ahluwalia A, Alexander SP, Giembycz MA *et al*. (2015). Experimental design and analysis and their reporting: new guidance for publication in BJP. Br J Pharmacol 172: 3461–3471.

Falanga V (2005). Wound healing and its impairment in the diabetic foot. Lancet 366: 1736–1743.

Ferrara N (2009). VEGF-A: a critical regulator of blood vessel growth. Eur Cytokine Netw 20: 158–163.

Ferrara N (2010). Pathways mediating VEGF-independent tumor angiogenesis. Cytokine Growth Factor Rev 21: 21–26.

Galeano M, Altavilla D, Cucinotta D, Russo GT, Calò M, Bitto A *et al*. (2004). Recombinant human erythropoietin stimulates angiogenesis and wound healing in the genetically diabetic mouse. Diabetes 53: 2509–2517.

Galeano M, Bitto A, Altavilla D, Minutoli L, Polito F, Calò M *et al*. (2008). Polydeoxyribonucleotide stimulates angiogenesis and wound healing in the genetically diabetic mouse. Wound Repair Regen 16: 208–217.

Gandellini P, Profumo V, Folini M, Zaffaroni N (2011). MicroRNAs as new therapeutic targets and tools in cancer. Expert Opin Ther Targets 15: 265–279.

Hu SC, Lan CE (2016). High-glucose environment disturbs the physiologic functions of keratinocytes: focusing on diabetic wound healing. J Dermatol Sci 84: 121–127.

Ishida M, Selaru FM (2013). miRNA-based therapeutic strategies. Curr Anesthesiol Rep 1: 63–70.

Johnson KE, Wilgus TA (2014). Vascular endothelial growth factor and angiogenesis in the regulation of cutaneous wound repair. Adv Wound Care (New Rochelle) 3: 647–661.

Kaeuferle T, Bartel S, Dehmel S, Krauss-Etschmann S (2014). MicroRNA methodology: advances in miRNA technologies. Methods Mol Biol 1169: 121–130.

Kilkenny C, Browne WJ, Cuthill IC, Emerson M, Altman DG (2010). Improving bioscience research reporting: the ARRIVE guidelines for reporting animal research. J Pharmacol Pharmacother 1: 94–99.

Kim KA, Shin YJ, Kim JH, Lee H, Noh SY, Jang SH *et al.* (2012). Dysfunction of endothelial progenitor cells under diabetic conditions and its underlying mechanisms. Arch Pharm Res 35: 223–234.

Krock BL, Skuli N, Simon MC (2011). Hypoxia-induced angiogenesis: good and evil. Genes Cancer 2 (12): 1117–1133.

Laganà A, Shasha D, Croce CM (2014). Synthetic RNAs for gene regulation: design principles and computational tools. Front Bioeng Biotechnol 2: 65.

Leeper NJ, Cooke JP (2011). MicroRNA and mechanisms of impaired angiogenesis in diabetes mellitus. Circulation 123: 236–238.

McGrath JC, Lilley E (2015). Implementing guidelines on reporting research using animals (ARRIVE etc.): new requirements for publication in BJP. Br J Pharmacol 172: 3189–3193.

Obad S, dos Santos CO, Petri A, Heidenblad M, Broom O, Ruse C *et al.* (2011). Silencing of microRNA families by seed-targeting tiny LNAs. Nat Genet 43: 371–378.

Peplow PV, Baxter GD (2012). Gene expression and release of growth factors during delayed wound healing: a review of studies in diabetic animals and possible combined laser phototherapy and growth factor treatment to enhance healing. Photomed Laser Surg 30: 617–636.

Peppa M, Raptis SA (2011). Glycoxidation and wound healing in diabetes: an interesting relationship. Curr Diabetes Rev 7: 416–425.

Poliseno L, Tuccoli A, Mariani L, Evangelista M, Citti L, Woods K *et al.* (2006). MicroRNAs modulate the angiogenic properties of HUVECs. Blood 108: 3068–3071.

Raffort J, Hinault C, Dumortier O, Van Obberghen E (2015). Circulating microRNAs and diabetes: potential applications in medical practice. Diabetologia 58: 1978–1992.

Russo GT, Di Benedetto A, Magazzù D, Giandalia A, Giorda CB, Ientile R *et al.* (2011). Mild hyperhomocysteinemia, C677T polymorphism on methylenetetrahydrofolate reductase gene and the risk of macroangiopathy in type 2 diabetes: a prospective study. Acta Diabetol 48: 95–101.

Shibuya M (2006). Differential roles of vascular endothelial growth factor receptor-1 and receptor-2 in angiogenesis. J Biochem Mol Biol 39: 469–478.

Sinha M, Ghatak S, Roy S, Sen CK (2015). microRNA-200b as a switch for inducible adult angiogenesis. Antioxid Redox Signal 22: 1257–1272.

Southan C, Sharman JL, Benson HE, Faccenda E, Pawson AJ, Alexander SPH *et al.* (2016). The IUPHAR/BPS guide to PHARMACOLOGY in 2016: towards curated quantitative interactions between 1300 protein targets and 6000 ligands. Nucl Acids Res 44: D1054–D1068.

Staton CA, Valluru M, Hoh L, Reed MW, Brown NJ (2010). Angiopoietin-1, angiopoietin-2 and Tie-2 receptor expression in human dermal wound repair and scarring. Br J Dermatol 163: 920–927.

Voglova K, Bezakova J, Herichova I (2016). Micro RNAs: an arguable appraisal in medicine. Endocr Regul 50: 106–124.

Wahl ML, Moser TL, Pizzo SV (2004). Angiostatin and anti-angiogenic therapy in human disease. Recent Prog Horm Res 59: 73–104.

Wang JM, Qiu Y, Yang ZQ, Li L, Zhang K (2017). Inositol-requiring enzyme 1 facilitates diabetic wound healing through modulating MicroRNAs. Diabetes 66: 177–192.

Wietecha MS, Di Pietro LA (2013). Therapeutic approaches to the regulation of wound angiogenesis. Adv Wound Care (New Rochelle) 2: 81–86.

Xu J, Zgheib C, Hu J, Wu W, Zhang L, Liechty KW (2014). The role of microRNA-15b in the impaired angiogenesis in diabetic wounds. Wound Repair Regen 22: 671–677.